

Research on the cooperative train control method in the metro system for energy saving

The
cooperative
train control
method

371

Siyao Li

*Railway Science and Technology Research and Development Center,
China Academy of Railway Sciences Corporation Limited, Beijing, China*

Bo Yuan

*Transportation Research Center,
Beijing Urban Construction Design & Research Institute Co., Ltd, Beijing, China*

Yun Bai

*School of Traffic and Transportation, Beijing Jiaotong University,
Beijing, China, and*

Jianfeng Liu

*Transportation Research Center,
Beijing Urban Construction Design & Research Institute Co., Ltd, Beijing, China*

Received 14 July 2023
Revised 12 August 2023
Accepted 16 August 2023

Abstract

Purpose – To address the problem that the current train operation mode that train selects one of several offline pre-generated control schemes before the departure and operates following the scheme after the departure, energy-saving performance of the whole metro system cannot be guaranteed.

Design/methodology/approach – A cooperative train control framework is formulated to regulate a novel train operation mode. The classic train four-phase control strategy is improved for generating specific energy-efficient control schemes for each train. An improved brute force (BF) algorithm with a two-layer searching idea is designed to solve the optimisation model of energy-efficient train control schemes.

Findings – Case studies on the actual metro line in Guangzhou, China verify the effectiveness of the proposed train control methods compared with four-phase control strategy under different kinds of train operation scenarios and calculation parameters. The verification on the computation efficiency as well as accuracy of the proposed algorithm indicates that it meets the requirement of online optimisation.

Originality/value – Most existing studies optimised energy-efficient train timetable or train control strategies through an offline process, which has a defect in coping with the disturbance or delays effectively and promptly during real-time train operation. This paper studies an online optimisation of cooperative train control based on the rolling optimisation idea, where energy-efficient train operation can be realised once train running time is determined, thus mitigating the impact of unpredictable operation situations on the energy-saving performance of trains.

Keywords Train operation scheme, Energy saving, Cooperative control, Metro system

Paper type Research paper

© Siyao Li, Bo Yuan, Yun Bai and Jianfeng Liu. Published in *Railway Sciences*. Published by Emerald Publishing Limited. This article is published under the Creative Commons Attribution (CC BY 4.0) licence. Anyone may reproduce, distribute, translate and create derivative works of this article (for both commercial and non-commercial purposes), subject to full attribution to the original publication and authors. The full terms of this licence may be seen at <http://creativecommons.org/licenses/by/4.0/legalcode>

This research was supported by the National Natural Science Foundation of China (Grant No. 71971016). On behalf of all co-authors, the corresponding author states that there is no conflict of interest.



1. Introduction

By the end of 2022, 55 cities in China have operated metro lines with a total operating mileage of 10 287.45 kilometers (Urban Rail Transit, 2022 Annual Statistics and Analysis Report). In 2022, the energy consumption of urban rail transit in China was up to 22.792bn kWh, a 6.89% increase compared with the last year (Urban Rail Transit, 2022 Annual Statistics and Analysis Report).

In recent years, the emergence and popularisation of regenerative braking technique provide a new method for energy saving during train operation, which is the improvement of regenerative braking energy (RBE) utilisation to reduce net energy consumption. It is in line with the efficient usage of energy and has become an important research direction. In modern metro system with small headway, frequent traction and braking processes of trains are conducive to the generation and usage of RBE and thus reduce net energy consumption, as shown in Figure 1.

In general, the improvement of train RBE utilisation can be realised by three approaches: energy storage device usage, train timetable optimisation and cooperative train control optimisation. For cooperative control of multiple trains, research studies mainly focused on coordinating train control regimes with the given train dispatch to increase the overlap probability of train traction and braking, thus improving RBE utilisation and reducing net energy.

Li (2014) analysed operation interaction and influence among trains, then formulated the multiple train energy-efficient control optimisation model and found the globally optimal solution by using game theory. The method proposed by Sun, Cai, Hou, Zhang, and Dong (2014) realised the utilisation of surplus RBE by partial adjustment of train speed curves. On the bases of this, the author further studied the optimal distribution method of RBE with the help of augmented Lagrange function (Sun, Lu, and Dong, 2017). To stabilise the substation power system and increase the usage of RBE, Xun, Tang, Song, Wang, and Jia (2015) proposed an energy-saving train control model, where the rise of power grid voltage due to the brake of one train could trigger the adjustment of control regimes of adjacent trains. Tang, Wang, and Feng (2015) formulated the energy-saving optimisation model of train tracking scenario based on the equivalent circuit of power supply grid. The quadratic programming algorithm was used to find the optimal control regimes of two trains to coordinate traction and braking process. Same for the train tracking scenario, Chen, Mao, Bai, Chen, and Shi (2017) segmented the metro line based on ramp conditions and speed limit and then analysed the train control regime selection and operation time allocation for each section. On the basis, a nested genetic algorithm was developed to find the optimal train control scheme. Liu analysed the energy-saving performance of train four- and five-mode control strategies on two-train (Liu, Guo, & Yu, 2016) and three-train (Liu & Zhao, 2017) operation scenarios. Compared with

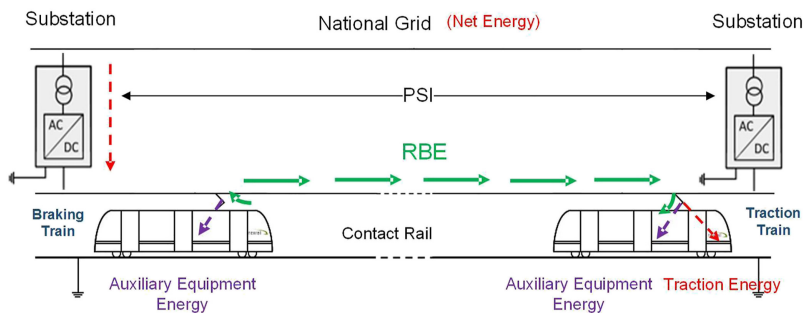


Figure 1.
The relationship of different kinds of energy in metro system

Source(s): Authors own work

train four-mode control strategy, the author added another acceleration phase into train control scheme to make full use of RBE generated by other braking trains. Similarly, based on substation power system, Jin, Feng, Sun, Chen, and Chai (2019) inserted a coasting-maximum acceleration phase into train control scheme to absorb RBE, but the assumption that train always runs with the speed as close as possible to the speed limit is not conducive for energy saving. The above-mentioned research studies mainly introduced general energy-efficient train control strategies but lacked the systematic framework and modelling. Bai *et al.* (2019) conducted a research on cooperative control of metro trains for minimising net energy consumption. The author applied cooperative co-evolutionary algorithm to generate control schemes of trains within a power supply region at one time, but the computation time of this method will remarkably rises with the increase of the number of trains. On the other hand, whether it is necessary to calculate all trains' control schemes simultaneously is still need to be deliberated since the efficiency of control schemes for non-decision trains may still be affected by the uncertainty during later practical operation (Bai, Yuan, Li, Zhou, & Feng, 2020; Ran *et al.*, 2022).

Existing studies on cooperative train control to reduce net energy consumption are still mainly offline optimisation process. The overall cooperative train control framework was rarely discussed. Therefore, this research is mainly focused on the online optimisation method of cooperative train control. A rolling optimisation idea is used when generating train control schemes to cope with the unpredictable conditions during practical operation, increasing train operational flexibility and robustness to some degree.

2. Cooperative train control method

2.1 Cooperative train control framework design

Cooperative train control is a sophisticated process, which has a demand on the centralised monitoring and dispatch. Based on the CBTC system, a cooperative train control framework is designed in this paper, as shown in Figure 2, where train control schemes are generated considering the operation status of other trains. It mainly consists of two levels, which are line CTC (centralised traffic control) and train OBCU (on-board control unit).

CTC level: line CTC receives real-time operation status of each train transmitted through the communication based train control system (CBTC) and sets up a shared database to store train control schemes. Then based on the database, the given running time, interstation line configuration, train data and the passenger flow at the station, CTC generates specific control schemes for each stopped train over time, forming a rolling optimisation process. The schemes aim at reducing net energy during train operation with the consideration of operation safety, comfort and punctuality. Finally, the control schemes will be transmitted through CBTC to each stopped train in real time.

OBCU level: the stopped train receives the control schemes from CTC. Then after departing from the station, onboard ATO precisely controls the train to operate at the next interstation following the given train control scheme.

2.2 Train control strategy

Under the above-mentioned cooperative train control framework, the specific energy-efficient control schemes for each train need to be determined. In this paper, the existing classic train four-phase control strategy is analysed and improved to some degree to increase the potential of energy saving.

2.2.1 *Four-phase control strategy.* It has been proved that train running on the route without steep downhill has minimum traction energy consumption by following four-phase control strategy (Lee, Milroy, & Tyler, 1982), which is maximum traction-coasting-

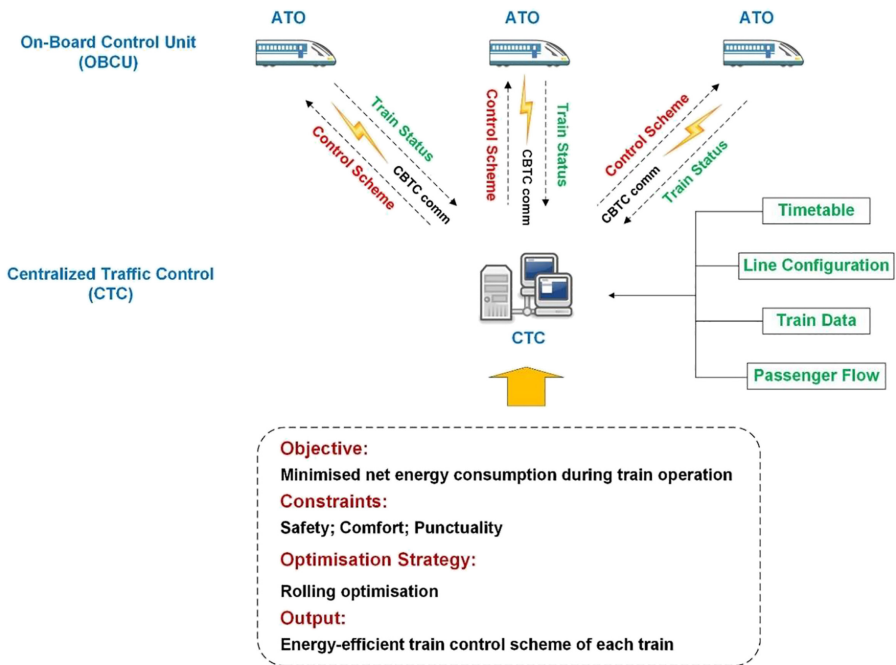


Figure 2.
Online cooperative
train control
framework

Source(s): Authors own work

maximum braking. As shown in Figure 3, as long as the final speed (v_{tr}) of train traction after the departure and the location (s_{co}) where train starts coasting before braking are given, the whole speed curve can be determined. It is noted that the location (s_{br}) where train starts braking is the intersect of train coasting curve (green line) and braking curve (blue line). In other words, once s_{co} and the terminus S are fixed, the above two curves will intersect at one point, which is s_{br} .

Typically, when train is cruising, it needs to apply partial traction or braking to maintain a constant cruising speed, specifically depending on the line conditions, train speed and train mass. As shown in Figure 4, if train is cruising on the uphill, the resultant force of train gravity and support force, which is the sliding force, is downward and parallel to the ramp. To

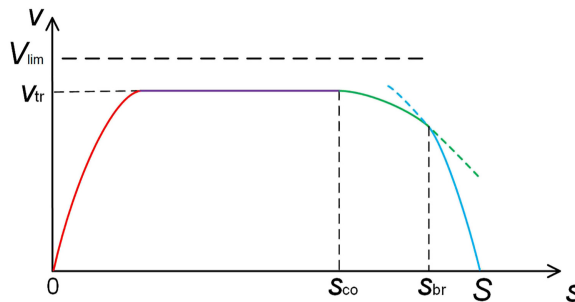
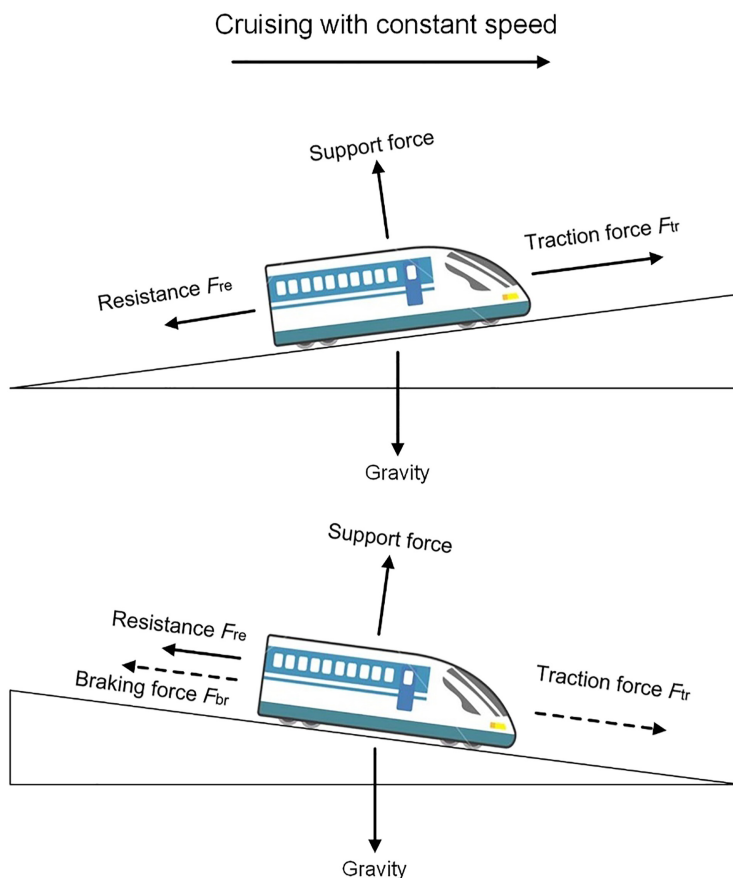


Figure 3.
Solution method of
speed curve of train
four-phase control
strategy

Source(s): Authors own work



Source(s): Authors own work

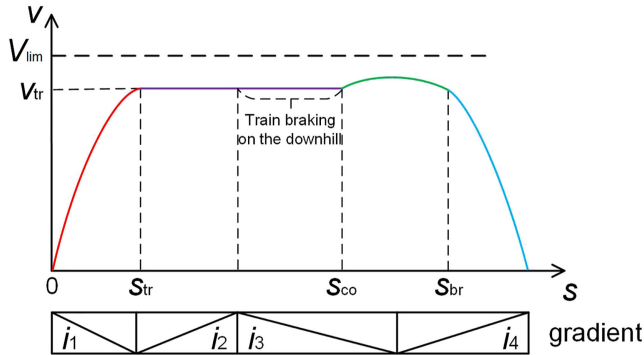
Figure 4. Force analysis during train cruising on the ramp

make the train run at a constant speed, that is the resultant force is zero, the train has to apply traction force to balance the resistance and sliding force.

While if train is cruising on the downhill, the sliding force is still downward, which can offset partial resistance. Therefore, when the sliding force is greater than the resistance, train has to apply braking force to balance the resultant force of resistance and sliding force. On the contrary, if the sliding force is smaller than the resistance, traction force is in need to offset the extra resistance.

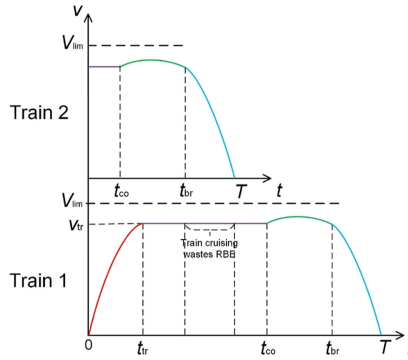
Based on the analysis above, for four-phase control strategy, if the train is cruising on the downhill, it may require braking to maintain the constant cruising speed as shown in Figure 5, which will cause train kinetic energy loss, thus increasing traction energy consumption. Specifically, for multiple-train operation scenario as shown in Figure 6, if a train is cruising when another train is braking, RBE generated by the braking train cannot be effectively used.

2.2.2 Improved control strategy. To address the above weaknesses of train four-phase control strategy under general line conditions and multiple-train operation scenarios, improvements are made as follows:



Source(s): Authors own work

Figure 5.
Train four-phase control strategy (single train scenario)



Source(s): Authors own work

Figure 6.
Train four-phase control strategy (multiple-train scenario)

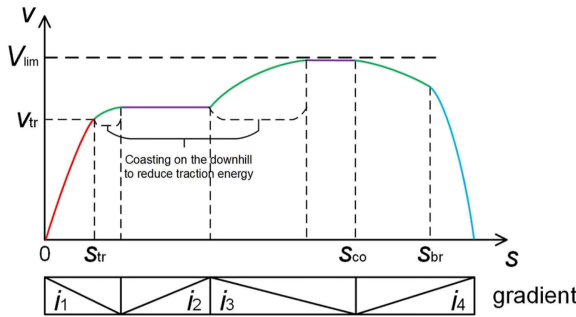
Improvement 1: for used during train running, to avoid train cruising on the downhill as much as possible, train control regime sequence can be improved as shown in Figure 7. The basic principle is that as long as train coasting on the ramp can speed up and not exceed the speed limit, it applies coasting, otherwise it applies cruising. This process can be realised by continuous judgement of train operation at each position between the interstation. Specific formula is as follows:

$$o(s + \Delta s) = \begin{cases} \text{Cruising, } [V_{\text{lim}}(s + \Delta s) - v(s) \cdot F_{\text{re}}[v(s), s + \Delta s] \geq 0 \\ \text{Coasting, } [V_{\text{lim}}(s + \Delta s) - v(s) \cdot F_{\text{re}}[v(s), s + \Delta s] < 0 \end{cases} \quad (1)$$

where

$o(s + \Delta s)$ denotes train control regime at location $s + \Delta s$;

$V_{\text{lim}}(s + \Delta s)$ denotes the speed limit at location $s + \Delta s$;



Source(s): Authors own work

Figure 7. Modified train control strategy (single train scenario)

$v(s)$ denotes train speed at location s and

$F_{re}[v(s), s + \Delta s]$ denotes train resistance at location $s + \Delta s$, which can be calculated by the following formula:

$$F_{re}[v(s), s + \Delta s] = [f_b(v(s)) + f_g(s + \Delta s) + f_c(s + \Delta s)] \cdot mg \quad (2)$$

where

m denotes the train mass;

g is gravitational acceleration;

$f_b(v(s))$ denotes the basic resistance when train speed is $v(s)$;

$f_b(s + \Delta s)$ denotes the resistance due to the ramp gradient at location $s + \Delta s$ and

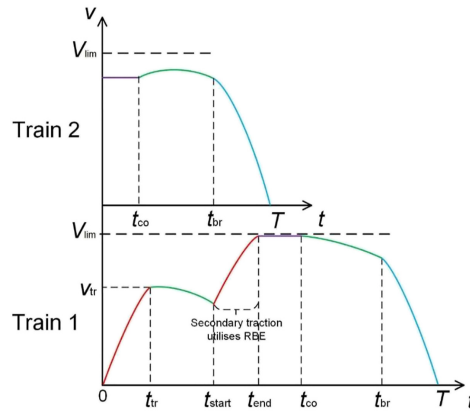
$f_c(s + \Delta s)$ denotes the resistance due to the line curve at location $s + \Delta s$.

This improvement can increase train kinetic energy by making full use of line ramp potential energy. In addition, once the train ends its first traction with v_{tr} departing from the station, its control regime at certain location is decided according to the current train operation status and line condition (no matter it's uphill, downhill or flat), which means the whole train speed curve can still be determined by v_{tr} and s_{co} . Therefore, compared with four-phase control strategy, the number of decision variables for generating the energy-efficient control scheme for one train is not increased by applying this improvement.

Improvement 2: for the cases of RBE utilisation among trains, to deal with the problem of RBE loss due to the fixed control regime sequence of train four-phase control strategy, multiple-traction is applied during train operation if necessary to use RBE generated by other braking trains as much as possible. As shown in Figure 8, when Train 2 is braking, Train 1 applies another traction phase to use RBE generated by Train 2.

Train operation status including speed curves, substation code as well as the energy consumption and generated RBE at each moment, etc. are stored in the shared database, where the time range whenever the surplus RBE can be used is known. Therefore, specific traction timing for the decision train can be determined based on the shared database. When

Figure 8.
Modified train control
strategy (multiple-train
scenario)



Source(s): Authors own work

generating speed curve for the decision train, the judgement will be made as the train moves to each position. If there is RBE which can be used during train running at the next distance step, the train will apply traction as long as it does not exceed the speed limit. Coasting is applied between the adjacent traction phases. Once train reaches the speed limit, it will not apply traction any more after that and strategy of Improvement 1 will be applied to determine the rest of train speed curve.

It is worth noting that in the above-mentioned method, the number of train tractions during operation is not restricted, which means if possible, the decision train can coordinate with multiple braking trains to use RBE. In addition, similar to Improvement 1, the number of decision variables for generating the whole train speed curve is still not increased when applying this improvement, since train speed curve between the location (s_{tr}) where train ends traction after the departure and the location (s_{co}) where train starts coasting before braking can be determined according to the shared database.

3. Model formulation

3.1 Assumptions

Mathematical optimisation model of energy-efficient train control formulated in this section is based on the following assumptions:

- (1) Train is regarded as a single mass point during model formulation. It has been proved (Howlett & Pudney, 1995) that train mass strip model can be transformed into single mass point model through ramp conversion. Therefore, single mass point model also has high accuracy and is applied in this study.
- (2) Train operation adopts two improved control strategies. That is for the cases of single train operation without RBE utilisation, the train applies the strategy of Improvement 1. If the train can use RBE generated by other trains, the strategies of Improvement 1 and 2 are adopted.

3.2 Decision variables

The decision variables of train control scheme between the interstation are the final speed of train traction after the departure and the location where train starts coasting before braking, which can be expressed as follows:

$$\phi = [v_{tr}, s_{co}] \quad (3)$$

where

ϕ represents train control scheme between the interstation;

v_{tr} denotes the final speed of train traction after departing from the station and

s_{co} denotes the location where train starts coasting before braking.

For train speed curve at other locations between the interstation, it can be determined by continuous judgement when generating train control schemes. According to the rolling optimisation theory, since during each optimisation process, only one control scheme for one train between an interstation is generated, the number of decision variables for model is not increased with the rise of the number of operating trains, which means the model solving efficiency can be guaranteed.

3.3 Objective function

The objective of the model in this paper is the minimisation of train net energy consumption during operation between each interstation, which can be expressed as follows:

$$\min E_{net}^i = E_{tr}^i - E_{RBE}^i = \int_0^T \left[e_{tr}^i(\phi) - \min \left(e_{tr}^i, \sum_{j \neq i}^N \alpha \cdot \beta \cdot e_{br}^j \right) \right] \cdot dt \quad (4)$$

$$e_{tr}^i = F_{tr}^i(v) \cdot v^i(t) + P_a \quad (5)$$

$$e_{br}^j = \max \left[\mu \cdot F_{br}^j(v) \cdot v^j(t) - P_a, 0 \right] \quad (6)$$

where

E_{net}^i denotes the net energy consumption of train i between the interstation;

E_{tr}^i denotes the traction energy consumption of train i between the interstation;

E_{RBE}^i denotes the amount of RBE that train i can use between the interstation;

T is the specified running time of train i between the interstation;

N is the number of trains in operation;

e_{tr}^i denotes the traction power of train i during dt ;

e_{br}^j denotes the regenerative braking power of train j during dt ;

P_a is the power of train onboard auxiliary equipment;

μ is the conversion factor from mechanical energy to RBE;

$v(t)$ denotes the train speed at time t and

α is a binary variable, whose value is

$$\alpha = \begin{cases} 1, & \text{Train } i \text{ and } j \text{ are in the same PSI} \\ 0, & \text{else} \end{cases} \quad (7)$$

β is a binary variable, whose value is

$$\beta = \begin{cases} 1, & F_{tr}^i(v) > 0 \text{ and } F_{br}^j(v) > 0 \text{ and } v^j(t) \geq V_c \\ 0, & \text{else} \end{cases} \quad (8)$$

V_c denotes the critical conversion speed of train regenerative braking and mechanical braking. When train speed is higher than V_c , it applies regenerative braking, generating RBE. When train speed is lower than V_c , it applies mechanical braking;

$F_{tr}(v)$ denotes train traction force when the speed is v , which can be obtained through train traction characteristic curve and

$F_{br}(v)$ denotes train braking force when the speed is v , which can be obtained through train braking characteristic curve.

Similarly, since train control schemes are gradually generated according to the practical operation conditions, each train runs between each interstation with the minimum energy consumption, ultimately minimising the net energy of the whole system.

3.4 Constraints

Some operation constraints need to be satisfied when generating train control schemes, which are as follows:

(1) Train movement equations

During train operation, kinematic equations should be followed. The train will be subjected to three kinds of forces: traction force, braking force and resistance, where the resistance consists of basic resistance as well as additional resistance due to line ramps and curves. Specific formulas are expressed as follows:

$$v(s) = \frac{ds}{dt} \quad (9)$$

$$a(s) = \frac{dv}{dt} = \frac{F_{tr}(v) - F_{br}(v)}{m} - f_{re}(v, s) \quad (10)$$

$$f_{re}(v, s) = f_b(v) + f_g(s) + f_c(s) \quad (11)$$

$$f_b(v) = a + bv + cv^2 \quad (12)$$

$$f_g(s) = -i(s) \quad (13)$$

$$f_c(s) = \frac{600}{r(s)} \quad (14)$$

where

$v(s)$ denotes train speed at location s ;

$a(s)$ denotes train acceleration at location s ;

m denotes the train mass between the interstation, which is determined based on the real-time trainload;

$f_{re}(v, s)$ denotes train unit resistance;

$f_b(v), f_g(s), f_c(s)$ are unit basic resistance, unit additional resistance due to line ramps and curves, respectively;

a, b, c are coefficients of Davis Equation [39], which are used to calculate basic resistance and provided by the rolling stock manufacturer;

$i(s)$ denotes the gradient of line ramp at location s and

$r(s)$ denotes the radius of line curve at location s .

(2) Punctuality

Trains have to run with the given running time between the interstation to guarantee the punctuality, which can be expressed as follows:

$$\left| \int_0^S \frac{\Delta s}{v(s)} \cdot ds - T \right| \leq \varepsilon \quad (15)$$

where

S denotes the distance between the interstation;

Δs denotes the distance step during calculation;

T denotes the specified running time between the interstation and

ε denotes a satisfying precision error of train running time.

(3) Traction rules

Since high speed before train arriving at the station is not conducive to slowing down and stopping, the time range of additional train tractions has to be restricted. In this study, it is achieved through no more train tractions after the certain moment, which is related to the running time between the interstation, as expressed in the following formula:

$$t_{\max_traction} \leq (1 - \lambda) T \quad (16)$$

where

$t_{\max_traction}$ denotes the moment after which train traction is not applied;

T is the specified running time between the interstation;

λ is a coefficient between 0 and 1.

(4) Train operation boundary constraints

To satisfy the exactness of stop, train has to be stationary before departing from the station and after arriving at the station, which can be represented as follows:

$$v(0) = v(S) = 0 \quad (17)$$

where

S is the distance between the interstation.

(5) Speed limit

To ensure safe operation, train speed has to be below the speed limit during train operation at all time, which can be expressed as follows:

$$v(s) \leq V_{\text{lim}}(s) \quad (18)$$

where

$v(s)$ is train speed at location s ;

$V_{\text{lim}}(s)$ is the speed limit at location s .

(6) Train tracking safety

Since multiple trains are running online at the same time, the operational interrelationships among them should be considered. The minimum safe distance between trains has to be satisfied at all time, which is expressed as follows:

$$|L^i(t) - L^{i-1}(t)| \geq \frac{v^i(t)^2}{a_{\text{eb}}} + l_s \quad (i > 1) \quad (19)$$

where

$L^i(t)$ denotes the location of train i at time t ;

$L^{i-1}(t)$ denotes the location of the previous train before train i at time t ;

$v(t)$ is train speed at time t ;

a_{eb} denotes the emergency braking deceleration of train and

l_s denotes a regulated fixed safety distance.

(7) Comfort

To meet the requirements of passenger ride comfort, train acceleration and deceleration during operation should be restricted as follows:

$$-b_{\text{max}} \leq a(s) \leq a_{\text{max}} \quad (20)$$

where

$a(s)$ is train acceleration at location s ;

b_{max} denotes the maximum train deceleration and

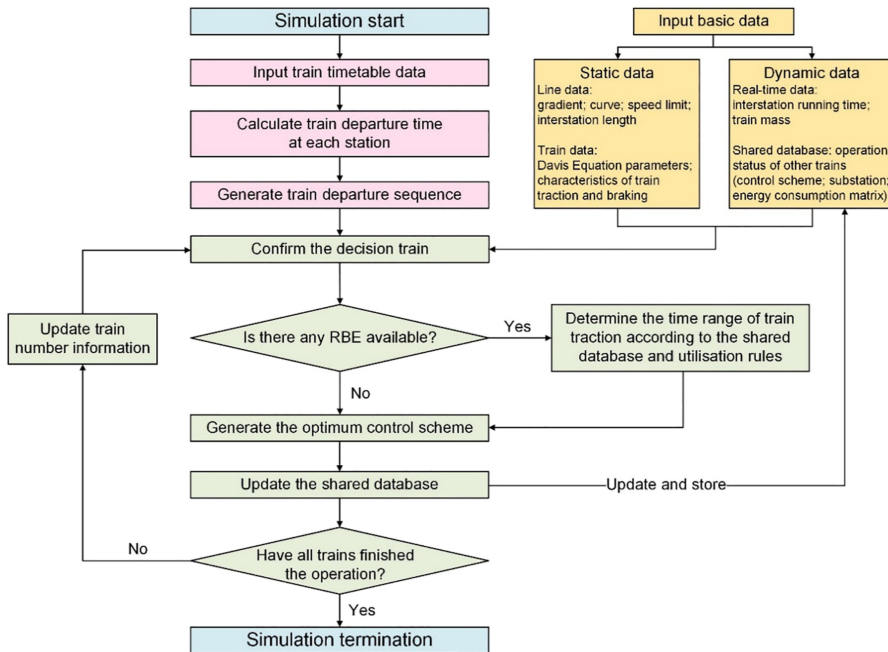
a_{max} denotes the maximum train acceleration.

4. Methodology

4.1 Simulation framework

To simulate the process of train control scheme generation by line CTC and the operation of multiple trains, a simulation framework is designed in this paper as shown in [Figure 9](#).

It should be noted that when generating train departure sequence, if there are more than one train departing at the same time, departure sequence at this time will be sorted according to the train number. Control schemes for each decision train at each interstation are gradually



Source(s): Authors own work

Figure 9. Simulation process of control scheme generation and train operation

generated according to train departure sequence. An improved brute force (BF) algorithm is adopted for searching the optimum train control scheme.

4.2 Improved brute force algorithm

BF algorithm is a kind of enumeration method, which searches all feasible solutions and chooses the best one. It has been adopted in many research studies in the field of train control optimisation (Zhao, Roberts & Hillmansen, 2014; Zhao, Roberts, Hillmansen & Nicholson, 2015; Zhou, Bai, Li, Mao & Li, 2018). It is clear that the solution space determines the computation time to some degree. Since train control schemes are generated online in this paper, computation efficiency has to be guaranteed.

In order to accomplish train control scheme optimisation within a satisfying time, an improved BF algorithm is proposed to increase the computation efficiency. Specifically, a two-layer searching idea is added into train control scheme searching process, which reduces the solution space to some extent. The searching procedure of the proposed improved BF algorithm is as follows:

Step 1: Algorithm initialisation. Input decision train data, line configuration, speed limit V_{lim} , running time T and the shared database which is in the matrix form to record train operation status and RBE generation of each time step. Initialize the final speed of train traction v_{tr} as 0, the train control scheme ϕ and the energy consumption E as empty set.

Step 2: Calculate and store train braking speed curve where train starts braking when the speed is V_{lim} as show in Figure 10.

Step 3: Search the shared database and determine whether RBE is available during train operation period. If it is available, train control scheme is generated base on the strategy of Improvement 1 and 2. Otherwise, train control scheme is generated base on strategy of Improvement 1.

Step 4: $v_{tr} = v_{tr} + 1$. If $v_{tr} > V_{lim}$, go to Step 6; Otherwise, generate train traction speed curve (red line) where the final speed is v_{tr} as shown in Figure 11. Then, calculate the speed curve after the end position (s_{tr}) of train traction following the corresponding strategies of Improvement 1 and 2 until it intersects with train braking curve (blue line) generated in Step 2, forming a complete train speed curve as shown in Figure 11, where train coasting before braking is not applied.

Step 5: Record the speed curve as $\phi_{no-co}(v_{tr})$ and calculate its running time $T_{no-co}(v_{tr})$ and then go to Step 4.

Step 6: Find the minimum v_{tr} where $|T_{no-co}(v_{tr}) - T| \leq \epsilon$ and then, record train control scheme $\phi(v_{tr}) = \phi_{no-co}(v_{tr})$ and calculate its energy consumption $E(v_{tr})$.

Step 7: $v_{tr} = v_{tr} + 1$. If $v_{tr} > V_{lim}$, go to Step 11; otherwise, search for s_{co} to meet the requirement of train running time T based on $\phi_{no-co}(v_{tr})$. To speed up the search process of the optimal s_{co} with the given v_{tr} , a two-layer searching idea is applied.

Step 8: First-layer search. Divide the distance between s_{tr_end} and s_{br} of $\phi_{no-co}(v_{tr})$ into P sections as shown in Figure 12a. Successively generate train speed curves with each split

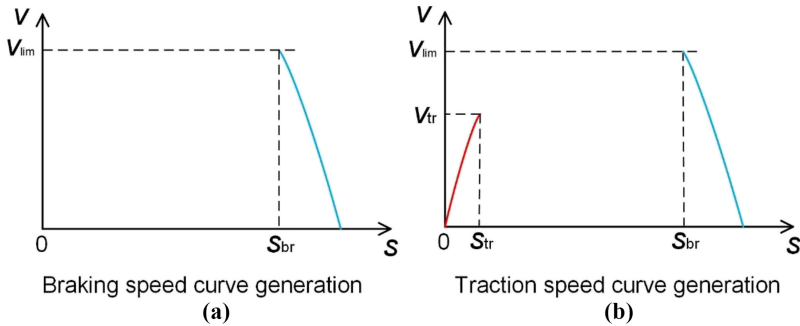


Figure 10. Generation of train braking speed curve and traction speed curve

Source(s): Authors own work

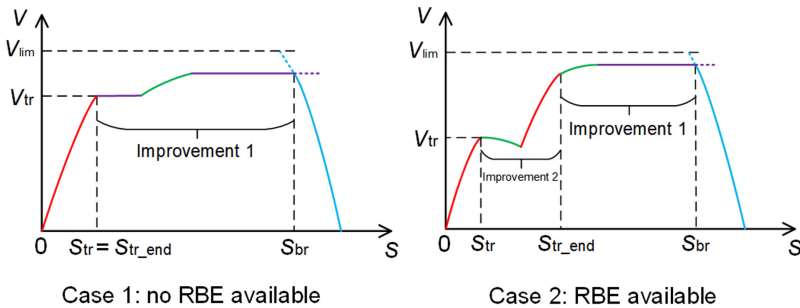
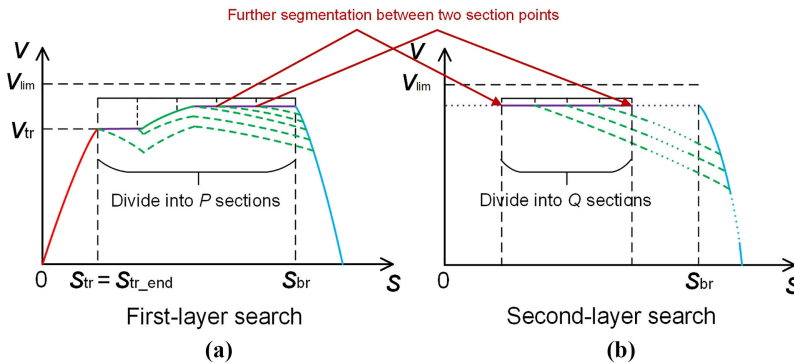


Figure 11. Generation of the whole train speed curve using Improvement 1 and 2

Source(s): Authors own work



Source(s): Authors own work

Figure 12. Two-layer search idea when generating train speed curves

point as s_{co} and calculate their running times. If there exists a split point s_{co} whose running time of speed curve meets the running time requirement, go to Step 10; Otherwise, find two split points whose running times of speed curves are at two sides of the giving running time T and then go to Step 9.

Step 9: Second-layer search. Further divide the distance between two split points selected in Step 8 into Q sections as shown in Figure 12b. Successively generate train speed curves with each split point as s_{co} and calculate their running times. Find one split point as the final s_{co} whose running time of speed curve meets the running time requirement. It should be noted that two-layer search is totally enough to find the optimal s_{co} for the metro system as the interstation is relatively short.

Step 10: Record train control scheme $\phi(v_{tr}, s_{co})$ and calculates its energy consumption $E(v_{tr})$ and then go to Step 7.

Step 11: Find one scheme from ϕ with the minimum energy consumption as the optimum train control scheme. Calculate RBE generation for each time step and store it as well as train speed curve in the shared database. Then terminate the algorithm until the next train sequence.

5. Case study and analysis

To verify the effectiveness of the proposed energy-efficient train control method and improved BF algorithm, a practical metro line in China is selected as the research object to conduct case studies. Energy-saving performance under different line conditions and train operation scenarios are analysed to explore the applicability of the proposed method.

5.1 Case data

Guangzhou metro line 2 as shown in Figure 13, which has a total length of 31.8 kilometers with 24 underground stations, is chosen for case studies in this paper. It is roughly a north-south line that runs from Guangzhou south railway station (GZSRS) to Jiahewanggang (JHWG) station. Since the implementation of the proposed methods is not affected by train running directions, the north-bound operation direction of line is selected during the simulation process. Basic line data, timetable, rollingstock parameters and simulation parameters are shown as follows:

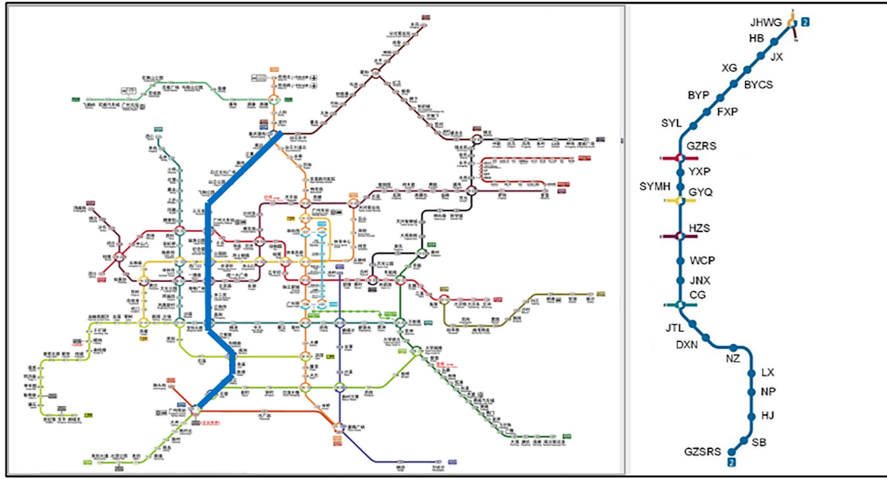


Figure 13.
Map of Guangzhou metro line 2

Source(s): Guangzhou Metro Map (2023)

(1) Line configuration

The length between each interstation and subsections of Guangzhou metro line 2 are given in [Table 1](#). Line ramp and curve configurations are shown in [Figure 14](#).

(2) Train data

Train data in the simulation are partially referred to the practical operating attributes of trains on Guangzhou metro line 2, which are given in [Table 2](#) and [Figure 15](#).

Interstation code	Interstation name	Length/m	PSI code
1	GZRS-SB	1,036	1
2	SB-HJ	2,374	
3	HJ-NP	2,433	
4	NP-LX	1,194	
5	LX-NZ	2,411	2
6	NZ-DXN	902	
7	DXN-JTL	1,975	
8	JTL-CG	906	
9	CG-JNX	872	3
10	JNX-WCP	1,063	
11	WCP-HZS	999	
12	HZS-GYQ	1,267	
13	GYQ-SYMH	785	
14	SYMH-YXP	875	4
15	YXP-GZRS	1,096	
16	GZRS-SYL	1,214	
17	SYL-FXP	1,330	
18	FXP-BYP	1,617	
19	BYP-BYCS	1,021	5
20	BYCS-XG	1,123	
21	XG-JX	1,445	
22	JX-HB	1,240	
23	HB-JHWG	1,759	

Table 1.
Line condition of north-bound Guangzhou metro line 2

Source(s): Authors own work

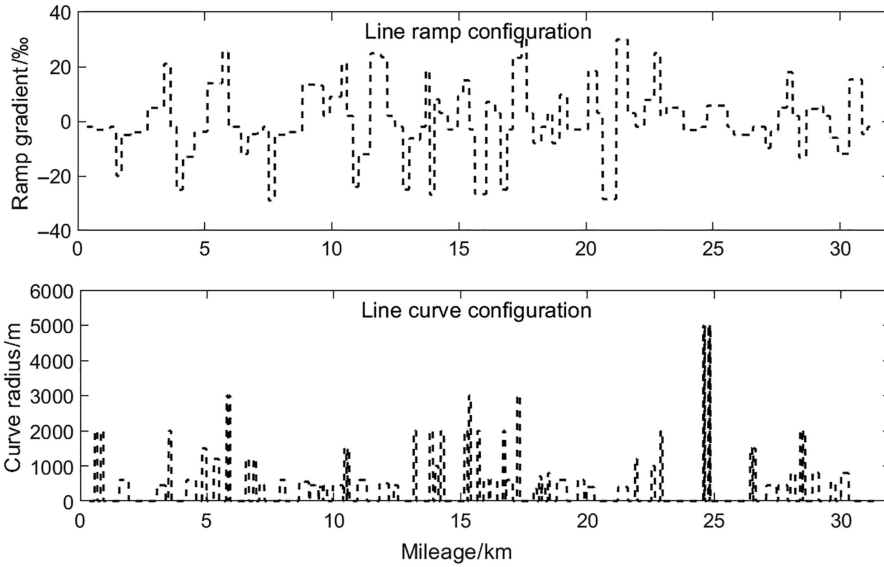


Figure 14. Ramp and curve configuration of north-bound Guangzhou metro line 2

Source(s): Authors own work

Title/Unit	Value	
Train type	A-type	
Marshalling	Tc-Mp-M-Mp-Tc	
Train mass m/t	335.4	
Train length/(safety distance) l_s/m	140	
Coefficients of Davis Equation	a	2.7551
	b	0
	c	0.0004286
Maximum acceleration $a_{max}/m/s^2$	1.0	
Maximum deceleration $b_{max}/m/s^2$	1.0	
Emergency braking deceleration $a_{eb}/m/s^2$	1.2	
Maximum speed/(Speed limit) $V_{lim}/km/h$	80	
Braking mode	Electric and mechanical	
Critical speed of electric and mechanical braking $V_c/km/h$	8	
Power of onboard auxiliary equipment P_a/kW	20	

Table 2. Train parameters in the simulation

Source(s): Authors own work

(3) Timetable

Train running time between each interstation and dwell time at each station of Guangzhou metro line 2 are given in Table 3.

(4) Computation parameters

Other parameters required during the simulation are given in Table 4.

5.2 Results

5.2.1 Energy-saving performance for single-train operation scenario. For single train operation scenario, the train runs following the strategy of Improvement 1. To verify the energy-saving

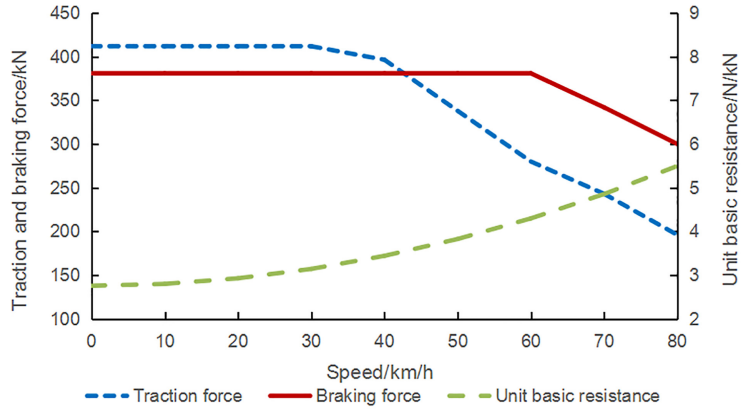


Figure 15. Characteristics of train traction, braking and unit basic resistance

Source(s): Authors own work

Station code	Station name	Running time/s	Dwelling time/s
1	GZSRS	78	0
2	SB	140	48
3	HJ	145	48
4	NP	86	48
5	LX	145	48
6	NZ	73	49
7	DXN	126	50
8	JTL	77	35
9	CG	73	55
10	JNX	82	45
11	WCP	79	50
12	HZS	97	55
13	GYQ	72	55
14	SYMH	72	49
15	YXP	84	45
16	GZRS	89	55
17	SYL	102	35
18	FXP	106	39
19	BYP	89	39
20	BYCS	84	39
21	XG	103	39
22	JX	89	39
23	HB	129	40
24	JHWG	-	0

Table 3. Train timetable parameters in the simulation

Source(s): Authors own work

effect of this proposed modified train control method compared with four-phase control strategy, one single train operation on the whole line with different control strategies is taken as an example. Simulation results including train speed curves, energy consumption, computation time, etc., are given in Figure 16 and Table 5.

Title/Unit	Value
Gravitational acceleration $g/m/s^2$	9.8
Distance step $\Delta s/m$	5
Conversion factor μ	0.9
Running time precision error e/s	0.5
Coefficient λ	0.4
Number of segments in first-layer search P	8
Number of segments in first-layer search Q	5

Source(s): Authors own work

Table 4. Other required parameters in the simulation

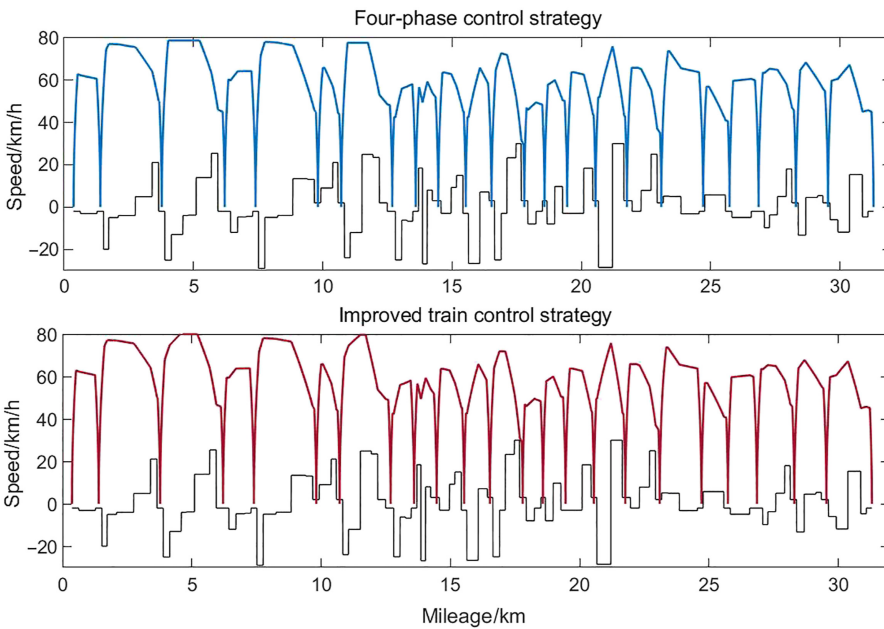


Figure 16. Train speed curves under different control strategies

Source(s): Authors own work

Title/Unit	Four-phase control	Improved control
Traction energy/kWh	378.5	369.8
Generated RBE/kWh	214.4	205.3
Used RBE/kWh (by onboard auxiliary equipment)	1.8	1.5
RBE utilisation rate	0.84%	0.73%
Net energy/kWh	376.7	368.3
Energy-saving rate	–	2.23%
Average computation time at each interstation/s	0.75	0.83

Source(s): Authors own work

Table 5. Simulation results of train operation under different control strategies

In Figure 16, it can be seen train speed curves under two control strategies between the same interstation are almost the same except for a few interstations (e.g. interstation 3 and 7). The conclusion can be drawn from Table 5 that for single train operation scenario, compared with four-phase control strategy, train net energy consumption is reduced by 2.23% when train applies the proposed improved control strategy. Apart from that, since the improved strategy avoids train braking as much as possible, total generated RBE under this strategy is relatively lower than that under four-phase control strategy and correspondingly RBE utilisation is much lower. As for computation efficiency, the average computation time at each interstation applying both strategies is at a satisfying level, meeting the requirement of online optimisation.

5.2.2 *Energy-saving performance under different line conditions.* Based on the above analysis, it is clear that line ramp configuration has an obvious impact on energy-saving performance of the strategy of Improvement 1, since the gradient of line ramp affects the choice of train control regime at each position, thus influencing energy consumption during train operation.

In order to explore the energy-saving effect of the improved control strategy during train operation under different line ramp configurations, a ramp coefficient δ is adopted to transform the practical line into several virtual lines with different ramp configurations. Concretely, ramp gradient of virtual lines is calculated by multiplying coefficient δ to the ramp gradient of the original line which is the same as the setting in Figure 14.

It can be seen from Figure 17 that as the ramp coefficient δ increases, train energy consumption under four-phase control strategy presents a growing tendency since steeper downhill causes more kinetic energy loss during train cruising. While the case for the improved strategy shows the opposite pattern since more potential energy can be used when train applies coasting. Similarly, the energy-saving rate of the improved strategy compared with four-phase control strategy is rising as δ increases, and the average value under different line ramp conditions can be up to 3.23%.

The conclusion can be drawn from the above results that the proposed improved train control strategy has better energy-saving performance under different line ramp configurations compared with four-phase control strategy. In addition, the greater line ramp fluctuation, the more obvious the energy-saving effect, which means the proposed method is more applicable for train running on the general line conditions.

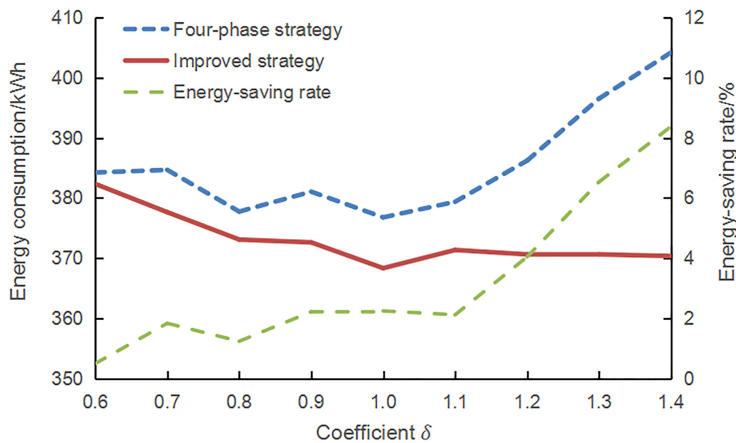


Figure 17. Energy-saving performance under different line ramp configurations

Source(s): Authors own work

5.2.3 Energy-saving performance for multi-train operation scenario. Different from single train operation, trains can utilise RBE from each other to reduce net energy consumption under multi-train operation scenario. In this section, three trains running in the same direction on the whole line with 180s of headway are taken for example to reflect energy-saving performance of the proposed train control method. Simulation results of train operation with different control strategies and train speed curves under the improved control strategy are given in [Table 6](#) and [Figure 18](#).

Although the modified control strategy with Improvement 1 (improved strategy in previous sections) has certain energy-saving effect compared with four-phase control strategy, RBE utilisation among trains is not fully considered. While train adopts the modified strategy with Improvement 1 and 2, although the total train traction energy consumption slightly increases compared with four-phase control strategy, used RBE rises dramatically, causing a significant reduction of net energy consumption of 5.59% and a 16.19 (29.01–12.82)% higher RBE utilisation rate. Compared with the modified strategy with Improvement 1, train net energy consumption is still reduced by 3.23%.

5.2.4 Energy-saving performance under different headways. Train headway has a direct impact on the net energy consumption of multi-train operation, since it determines the timing of traction and braking coordination among trains. The energy-saving effect of the proposed train control method is shown as [Figure 19](#).

Although for four-phase control strategy, the traction phase after the departure can be prolonged to some extent to use RBE generated by other trains, RBE utilisation is quite limited due to the fixed control regime sequence, which indicates the necessity of train control regime sequence modification. Apparently, for multiple-train operation under different headways, both two kinds of modified train control strategies have energy-saving effect compared with four-phase control strategy, and train net energy consumption can be reduced by 2.89 and 4.91% on average, respectively.

While, in [Figure 19](#), for several cases under certain headways, the energy-saving effect of the modified strategy of Improvement 1 is better than the case for the modified strategy of Improvement 1 and 2, which means in some situations, train consumes less energy during operation without multiple-traction phase. This phenomenon may happen where train has two traction phases with a large interval, and the secondary traction duration is relatively short. The reason is that long-distance coasting between tractions may significantly reduce train speed, causing the train to extend traction duration after the departure, thus increasing energy consumption to some degree.

Title/Unit	Four-phase control	Modified control with improvement 1	Modified control with improvement 1 and 2
Traction energy/kWh	1138.5	1105.8	1206.1
Generated RBE/kWh	647.6	625.1	722.4
Used RBE/kWh	83.0	76.0	209.6
RBE utilisation rate	12.82%	12.16%	29.01%
Net energy/kWh	1055.5	1029.8	996.5
Energy-saving rate	–	2.43%	5.59%/3.23%
Average computation time at each interstation/s	0.70	0.91	0.95

Source(s): Authors own work

Table 6.
Simulation results of
multi-train operation
scenario

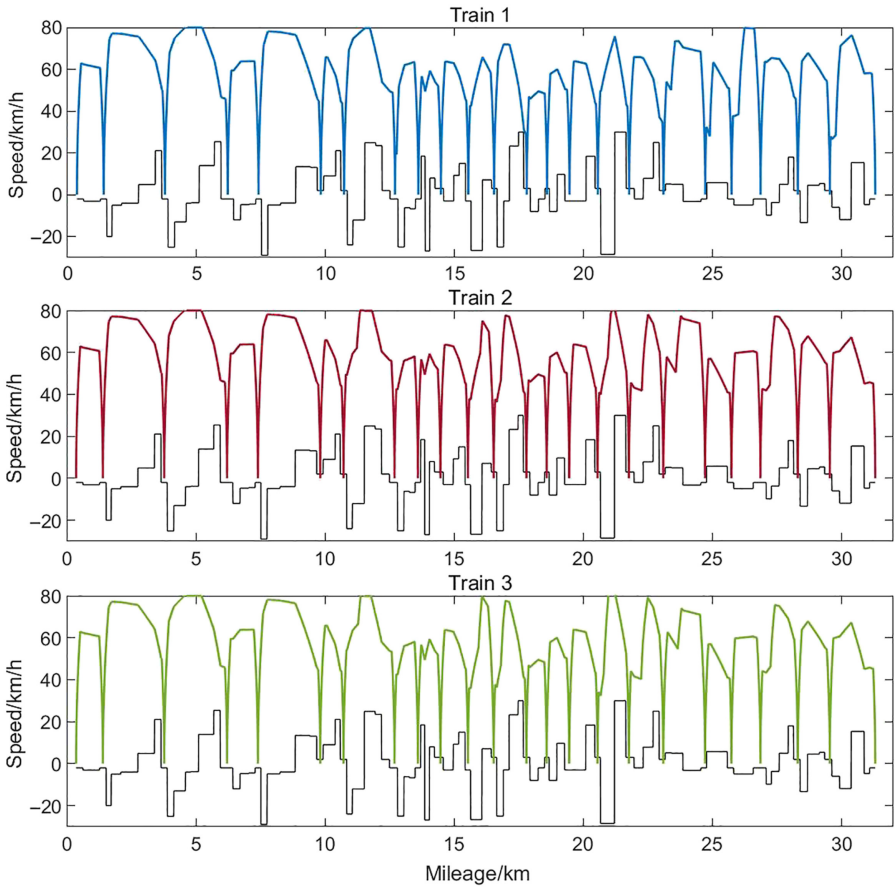


Figure 18.
Train speed curves under the modified strategy with Improvement 1 and 2

Source(s): Authors own work

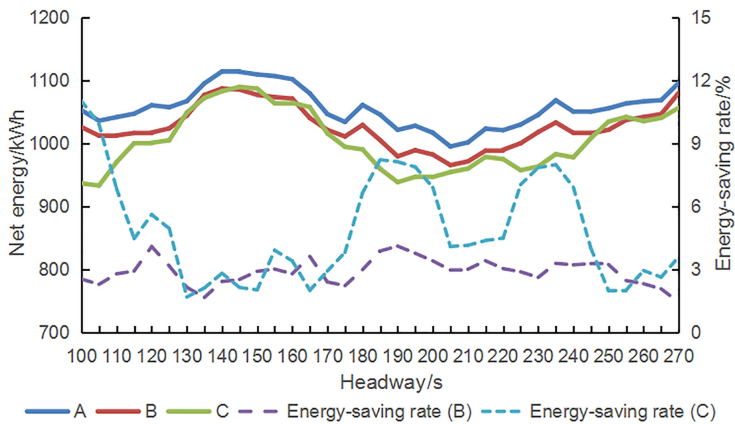


Figure 19.
Energy-saving effect of the proposed strategies under different headways

Source(s): Authors own work

6. Conclusion

In order to alleviate the rapidly increasing energy consumption in metro system, online cooperative train control method for energy saving is studied in this paper. A rolling optimisation idea of train control schemes is proposed to cope with the impact of practical train operating situations on the energy-saving performance of the existing offline optimisation methods. Compared with the current train operation mode where train control schemes are offline pre-generated and online selected according to actual conditions, the proposed train control method has higher operation flexibility and robustness when dealing with the unpredictable disturbance. Case studies on a real metro line in Guangzhou, China are conducted to verify the effectiveness of the proposed train control method and algorithm. Conclusions that can be drawn from case studies are as follows:

- (1) For single-train operation scenario, the modified train control strategy in this study is more applicable under general line conditions compared with train four-phase control strategy, since it allows the train to make the best possible use of ramp potential energy to speed up, thus reducing traction energy consumption. The average energy-saving rate under different line ramp configurations can be up to 3.23%.
- (2) For multi-train operation scenario, according to the proposed modified train control method, trains are allowed to apply multiple-traction to absorb RBE generated by other adjacent braking trains. The train net energy saving effect can be achieved under different headways compared with the case where train adopts four-phase control strategy, and the net energy can be reduced by 4.91% on average.
- (3) The proposed improved BF algorithm can meet the requirement of online calculation accuracy and efficiency, where the two-layer searching idea effectively reduces the computation time with a satisfying solution quality compared with conventional searching strategies.

References

- Bai, Y., Cao, Y., Yu, Z., Ho, T. K., Roberts, C., & Mao, B. (2019). Cooperative control of metro trains to minimize net energy consumption. *IEEE Transactions on Intelligent Transportation Systems*, 21(5), 2063–2077.
- Bai, Y., Yuan, B., Li, J., Zhou, Y., & Feng, X. (2020). Cooperative control strategy for energy saving operation of metro train based on rolling optimization. *China Railway Sciences*, 41(3), 163–170.
- Chen, Z., Mao, B., Bai, Y., Chen, S., & Shi, R. (2017). Optimization on energy-efficient operations for trailing train in urban rail system with fixed run-time. *Journal of the China Railway Society*, 39(8), 10–17.
- Howlett, P., & Pudney, P. (1995). *Energy-efficient train control*. London: Springer.
- Jin, B., Feng, X., Sun, P., Chen, M., & Chai, Y. (2019). Energy saving in metro transit substation through train trajectory optimization. In *2019 IEEE Intelligent Transportation Systems Conference (ITSC)* (pp. 2829–2834).
- Lee, D. H., Milroy, I. P., & Tyler, K. (1982). Application of Pontryagin's maximum principle to the semi-automatic control of rail vehicles. In *Second Conference on Control Engineering 1982: Merging of Technology and Theory to Solve Industrial Automation Problems*. Institution of Engineers.
- Li, K. (2014). *The study on energy saving optimization method of multi-train cooperative control*. Beijing Jiaotong University.
- Liu, J., & Zhao, N. (2017). Research on energy-saving operation strategy for multiple trains on the urban subway line. *Energies*, 10(12), 2156.

- Liu, J., Guo, H., & Yu, Y. (2016). Research on the cooperative train control strategy to reduce energy consumption. *IEEE Transactions on Intelligent Transportation Systems*, 18(5), 1134–1142.
- Ran, X., Chen, S., Bai, Y., Chen, Y., Chen, Z., & Yang, C. (2022). Train energy-efficient and passenger time-saving timetable optimization model for urban rail transit line with tidal passenger flow. *China Railway Sciences*, 43(1), 171–181.
- Sun, X., Cai, H., Hou, X., Zhang, M., & Dong, H. (2014). Regenerative braking energy utilization by multi train cooperation. In *17th International IEEE Conference on Intelligent Transportation Systems (ITSC)*, 2014 (pp. 139–144).
- Sun, X., Lu, H., & Dong, H. (2017). Energy-efficient train control by multi-train dynamic cooperation. *IEEE Transactions on Intelligent Transportation Systems*, 18(11), 3114–3121.
- Tang, H., Wang, Q., & Feng, X. (2015). Energy saving control of metro train tracing operation. *Journal of the China Railway Society*, 37(1), 37–43.
- Urban Rail Transit (2022). *Annual Statistics and analysis Report*. China Association of Metros. Available from: <https://www.camet.org.cn/tjxx/11944> (accessed 31 March 2023).
- Xun, J., Tang, T., Song, X., Wang, B., & Jia, Z. (2015). Comprehensive model for energy-saving train operation of urban mass transit under regenerative brake. *China Railway Sciences*, 36(1), 104–110.
- Zhao, N., Roberts, C., & Hillmansen, S. (2014). The application of an enhanced brute force algorithm to minimise energy costs and train delays for differing railway train control systems. *Proceedings of the Institution of Mechanical Engineers, Part F: Journal of Rail and Rapid Transit*, 228(2), 158–168.
- Zhao, N., Roberts, C., Hillmansen, S., & Nicholson, G. (2015). A multiple train trajectory optimization to minimize energy consumption and delay. *IEEE Transactions on Intelligent Transportation Systems*, 16(5), 2363–2372.
- Zhou, Y., Bai, Y., Li, J., Mao, B., & Li, T. (2018). Integrated optimization on train control and timetable to minimize net energy consumption of metro lines. *Journal of Advanced Transportation*, 2018, 1–19. doi: [10.1155/2018/7905820](https://doi.org/10.1155/2018/7905820).

Further reading

- Davis, W. J. (1926). *The tractive resistance of electric locomotives and cars*. London: The General Electric Co., Ltd.
- Guangzhou Metro Map (2023). Guangzhou Bendibao: China. Available from: <http://jt.gz.bendibao.com/news/20161229/226263.shtml> (accessed 26 June 2023).

Corresponding author

Jianfeng Liu can be contacted at: 405455223@qq.com